Journal of Clinical Neuroscience 21 (2014) 1033–1039

Contents lists available at ScienceDirect

Journal of Clinical Neuroscience

journal homepage: www.elsevier.com/locate/jocn

Laboratory Studies

Hypomyelinating leukodystrophy-associated missense mutant of FAM126A/hyccin/DRCTNNB1A aggregates in the endoplasmic reticulum

Yuki Miyamoto [a,1], Tomohiro Torii [a,1], Takahiro Eguchi [d], Kazuaki Nakamura [a], Akito Tanoue [a], Junji Yamauchi [a,b,c,*]

[a] Department of Pharmacology, National Research Institute for Child Health and Development, 2-10-1 Okura, Setagaya, Tokyo 157-8535, Japan
[b] Graduate School of Medical and Dental Sciences, Tokyo Medical and Dental University, Bunkyo, Tokyo, Japan
[c] Japan Health Sciences Foundation, Chuo, Tokyo, Japan
[d] The Institute of Medical Science, The University of Tokyo, Minato, Tokyo, Japan

ARTICLE INFO

Article history:
Received 12 February 2013
Accepted 22 September 2013

Keywords:
Endoplasmic reticulum
FAM126A
Hypomyelinating leukodystrophy
Unfolded protein response

ABSTRACT

Hypomyelinating leukodystrophies (HLD) are hereditary central nervous system diseases in which the myelin sheath does not form properly. The disease prototype is the X-linked recessive Pelizaeus-Merzbacher disease (also now known as HLD1), which is caused by the mutation, multiplication, or deletion of the *plp1* gene. PLP1 missense mutations lead to protein aggregation and accumulation in subcellular compartments such as the endoplasmic reticulum (ER). The gene responsible for an autosomal recessive Pelizaeus-Merzbacher-like disease called HLD5 is named *fam126a* (also known as *hyccin* or *drctnnb1a*). While the gene mutations often cause FAM126A protein deficiency, one known missense mutation, Leu-53-to-Pro (L53P), allows some protein to be produced. Here, we show that the L53P mutant aggregates in cells, accumulating primarily in the ER. This is in contrast to the wild type FAM126A, which distributes throughout the cytoplasm. In addition, the L53P mutant expression promotes the activities of kinases involved in unfolded protein response. These results suggest that a disease-associated FAM126A missense mutation causes protein accumulation in subcellular compartments, possibly to mediate a disease-associated phenotype, which is similar to what is seen with PLP1.

1. Introduction

The myelin sheath is a unique multi-layer structure that acts as an insulator between surrounding axons [1]. The myelin sheath is derived from myelin-forming glial cells, which are called oligodendrocytes in the central nervous system (CNS) and Schwann cells in the peripheral nervous system. Over time, the myelin sheaths grow to more than one hundred times larger than the collective surface area of the premyelinating oligodendrocyte or Schwann cell plasma membranes [1].

Pelizaeus-Merzbacher disease is the prototypic hereditary hypomyelinating leukodystrophy (HLD) in oligodendrocytes [1–8]. In this disease (known as HLD1), missense PLP1 mutations generally cause protein aggregation, which results in accumulation of mutant PLP1 proteins in some subcellular compartments and triggers an unfolded protein response (UPR) [1–8]. Recent studies have identified other genes responsible for HLD (HLD2, HLD4, and HLD5) [9]. HLD5 (Mendelian Inheritance in Man number 610532) is a recessive disorder that causes hypomyelination and cataracts [10–12]. In most cases, HLD5 is caused by premature stop signal causing mutations in the *fam126a* (also known as *hyccin* or *drctnnb1a*) gene and FAM126A protein deficiency leads to neurological phenotypes such as intellectual disabilities and walking difficulties [10–12]. One unique *fam126a* gene mutation, which results in Leu-53-to-Pro (L53P), allows the FAM126A protein to be produced [10]. The aim of this study was to investigate whether this unique missense mutation changes the biochemical properties of FAM126A. We show, to our knowledge, for the first time, that the L53P mutation causes protein aggregation, similar to the missense mutations of PLP1. The protein accumulation primarily occurs in the endoplasmic reticulum (ER), stimulating UPR-responsible kinase activities.

2. Material and methods

2.1. Antibodies

The following antibodies were purchased: anti-calnexin (ER membrane marker protein) from Enzo Life Sciences (Farmingdale,

* Corresponding author. Tel.: +81 3 5494 7120x4670; fax: +81 3 5494 7057.
E-mail address: yamauchi-j@ncchd.go.jp (J. Yamauchi).
[1] These authors have contributed equally to the manuscript.

0967-5868/$ - see front matter © 2013 Elsevier Ltd. All rights reserved.
http://dx.doi.org/10.1016/j.jocn.2013.09.014

NY, USA); anti-Golgi matrix protein (GM) 130 from BD Biosciences Pharmingen (Franklin Lake, NJ, USA); anti-Lamp1 (lysosome marker protein) from Abcam (Cambridge, UK); anti-FLAG from Sigma-Aldrich (St. Louis, MO, USA); anti-eukaryotic translation initiation factor 2α subunit (eIF2α), anti-(pSer51) eIF2α (antibody specifically recognizing eIF2α phosphorylation through UPR), anti-pan c-Jun N-terminal kinase (JNK), and anti-pan (pThr183/Tyr185) JNK (antibody specifically recognizing active JNK) from Cell Signaling Technology (Beverly, MA, USA); peroxidase-conjugated secondary antibodies from GE Healthcare (Fairfield, CT, USA) and Nacalai Tesque (Kyoto, Japan); and fluorescence-labeled secondary antibodies from Life Technologies (Carlsbad, CA, USA) and Wako Pure Chemical Industries (Osaka, Japan).

2.2. Plasmids

The plasmid encoding FAM126A was purchased from Origene (Rockville, MD, USA). The polymerase chain reaction (PCR) amplified coding region was ligated into the pMEI5 vector (Takara Bio, Shiga, Japan) tagged with enhanced green fluorescent protein (EGFP) at the C-terminus and inserted into the pCMV5 vector tagged with FLAG at the C-terminus. The L53P variant, which was mutated with the overlapping PCR method, was also ligated into pMEI5-EGFP and pCMV-FLAG. The ER-mKeimaRed (ER-localization signal sequence-tagged modified RFP [red fluorescent protein]) plasmid was purchased from MBL (Nagoya, Japan). All DNA sequences were confirmed by the sequencing service of Fasmac (Kanagawa, Japan).

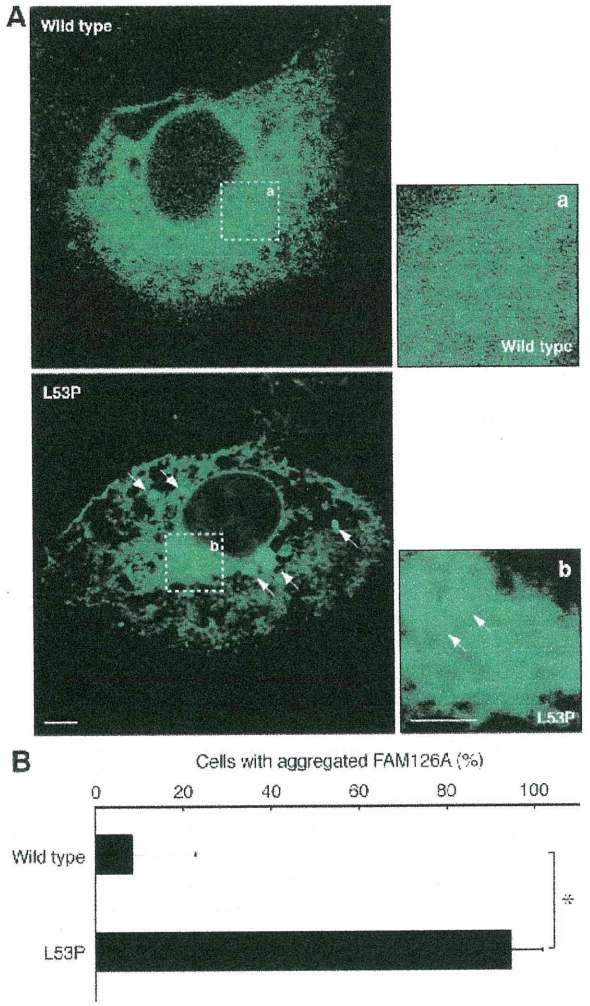

Fig. 1. Wild type FAM126A is present in the cytoplasm and the L53P mutant is in punctate structures. (A) Cos-7 cells were transfected with the plasmid encoding FAM126A-EGFP (a) or FAM126AL53P-EGFP (b). Scale bar = 10 μm. Arrows indicate typical large aggregate-like structure in cells transfected with the L53P mutant. (B) Cells with aggregate-like FAM126A proteins are shown as percentages of the total cells. The percentage of cells with aggregate-like FAM126A is significantly (*) higher in those transfected with the L53P mutant. (This figure is available in colour at www.sciencedirect.com.)

2.3. Cell culture and transfection

African green monkey kidney Cos-7 cells were cultured on dishes in Dulbecco's modified eagle's medium containing 10% fetal bovine serum, 50 U/ml penicillin, and 50 μg/ml streptomycin. The plasmid was transfected into Cos-7 cells using CalPhos Transfection Reagent (Takara Bio), according to the manufacturer's instruction. Cells were used for experiments 24 hours after transfection. Under these conditions, trypan blue-incorporating cells were less than 5% of the total cells.

2.4. Generation of transgenic mice

Genetically modified/unmodified mice were cared for in accordance with a protocol approved by the Japanese National Research Institute for Child Health and Development Animal Care Committee and were monitored by the Laboratory Animal Facility of the Japanese National Research Institute for Child Health and Development. Moloney murine leukemia virus (MoMLV) derived artificial intron was amplified using pMEI5 (901–1721 bases) as the template. The nucleotide units encoding simian virus 40 enhancer, mouse myelin basic protein (MBP) promoter (GenBank accession number JF429449), FLAG-tagged L53P variant of FAM126A, MoMLV intron, and human growth hormone polyA signal were successively inserted into a pCMV5 backbone as the subcloning vector. A DNA fragment (~5000 bases) containing all nucleotide units was digested from the vector backbone using *Sac*I and *Xho*I, purified, and injected into fertilized C57BL/6JJms oocytes. Transgenic (TG) founder mice and established TG mice were identified using tail genomic PCR with specific primers for two genes. The specific primer for the *sv40* enhancer was 5′-CCGGAATTCGAATATTAGCTAGGAGTTTCAGAAAGGGGGCCTG-3′ and 5′-CCGGAATTCACTAGTGGGACTATGGTTGCTGACTAATTGAGATGC-3′. The other specific primer was for the *flag-fam126al53p* gene, 5′-GAAAGAACCACAGACGGTCAGGAGGAAG-3′ and 5′-TTACTTGTCATCGTCATCCTTGTAATCGATGTCATGATC-3′. PCR was performed in 30 cycles, each consisting of denaturation at 94 °C for 1 minute, annealing at 62.5 °C for 1 minute, and extension at 72 °C for 1 minute. TG founders were mated to wild type C57BL/6JJms mice and the littermates were used for experiments. The TG mice as well as their non-TG littermates were fertile under standard breeding conditions. Male mice were used for experiments if it was possible to distinguish their sex.

2.5. Immunofluorescence

Cells on glass coverslips were fixed in phosphate buffered saline (PBS) containing 4% paraformaldehyde and permeabilized with PBS containing 0.1% Tween-20 [13,14]. Permeabilized cells were blocked with Blocking One (Nacalai Tesque), and incubated first with a primary antibody and then with fluorescence-labeled secondary antibodies. Fluorescence-labeled cells were preserved in a Vectashield reagent (Vector Laboratories, Burlingame, CA, USA) for microscope observation. The confocal images were collected using an IX81 microscope with a laser-scanning FV500 or FV1000D system (Olympus, Tokyo, Japan). Images were analyzed using FluoView software (Olympus). Cells with aggregated

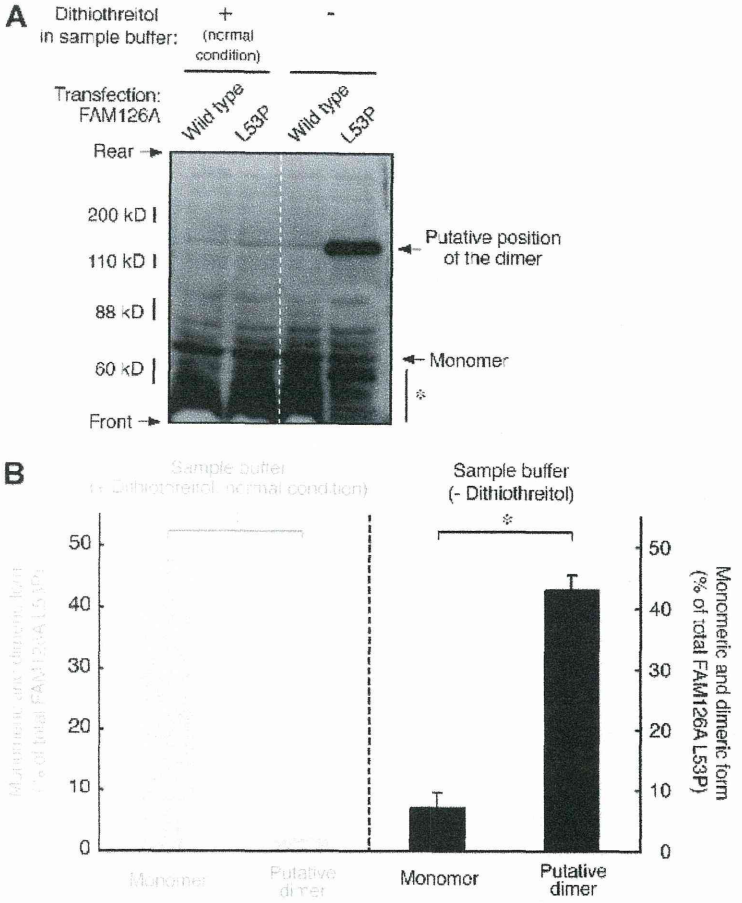

Fig. 2. The L53P mutant is a high molecular weight protein with disulfide bonds. (A) Asterisk indicates degradation products of transfected FAM126A. (B) Bands of monomeric and dimeric FAM126A proteins and their degradation products were scanned and the amount of monomeric and dimeric forms relative to the total protein was calculated as percentages. Left gray and right black bars indicate experiments in the presence and absence of dithiothreitol, respectively.

proteins were considered to have aggregates if their maximum fluorescent value was greater than 5000.

2.6. Immunohistochemistry

Tissues were perfused first with PBS and then with PBS containing 4% paraformaldehyde. They were postfixed with 4% paraformaldehyde, replaced with 20% sucrose, and embedded in Tissue-Tek reagent (Sakura Finetechnical, Tokyo, Japan). Microtome sections were blocked with Blocking One, and incubated first with primary antibodies and then with fluorescence-labeled secondary antibodies, and analyzed using confocal microscopy.

2.7. Immunoblotting

Cells or tissues were briefly sonicated in lysis buffer A (50 mM HEPES-NaOH, pH 7.5, 20 mM $MgCl_2$, 1 mM phenylmethane sulfonylfluoride, 1 μg/ml leupeptin, 1 mM ethylenediaminetetraacetic acid [EDTA], 1 mM Na_3VO_4, 10 mM NaF, 0.5% NP-40, 1% 3-[(3 cholamidopropyl)dimethylammonio]-1-propanesulfonate [CHAPS], and 0.3% sodium dodecyl sulfate [SDS]) on ice [13,14]. Proteins in the centrifugal supernatants were placed into sample buffer (50 mM Tris-HCl, pH 6.8, 2% SDS, and 10% glycerol) with or without 30 mM reducing agent dithiothreitol (No. 09499-14 or 09500-64, Nacalai Tesque) in boiled water for 5 minutes and applied to SDS-polyacrylamide gel electrophoresis (PAGE). The electrophoretically separated proteins were transferred to a polyvinylidene difluoride membrane, blocked with Blocking One, and immunoblotted with a primary antibody in the presence or absence of Blocking One. The bound peroxidase-conjugated secondary antibodies were detected using the chemiluminescence method. The scanned protein bands were analyzed densitometrically using UN-SCAN-IT software (Ryoka Systems, Tokyo, Japan).

2.8. Statistical analysis

Values shown represent the mean ± standard deviation from separate experiments. A one-way analysis of variance was followed by a Fisher's protected least significant difference test as a *post hoc* comparison. The p values less than 0.01 were generally considered significant.

3. Results

3.1. Expression of FAM126A L53P mutant in Cos-7 cells

The purpose of this study was to examine the effect of *fam126a* gene missense mutation on FAM126A protein properties. To investigate whether the L53P mutation of FAM126A protein has an effect on cellular localization, we transfected EGFP-tagged wild type or the L53P mutant construct into Cos-7 cells. Cos cell lines are widely utilized to determine the subcellular localization of various proteins, since they have large cell bodies [7,8,15]. We first

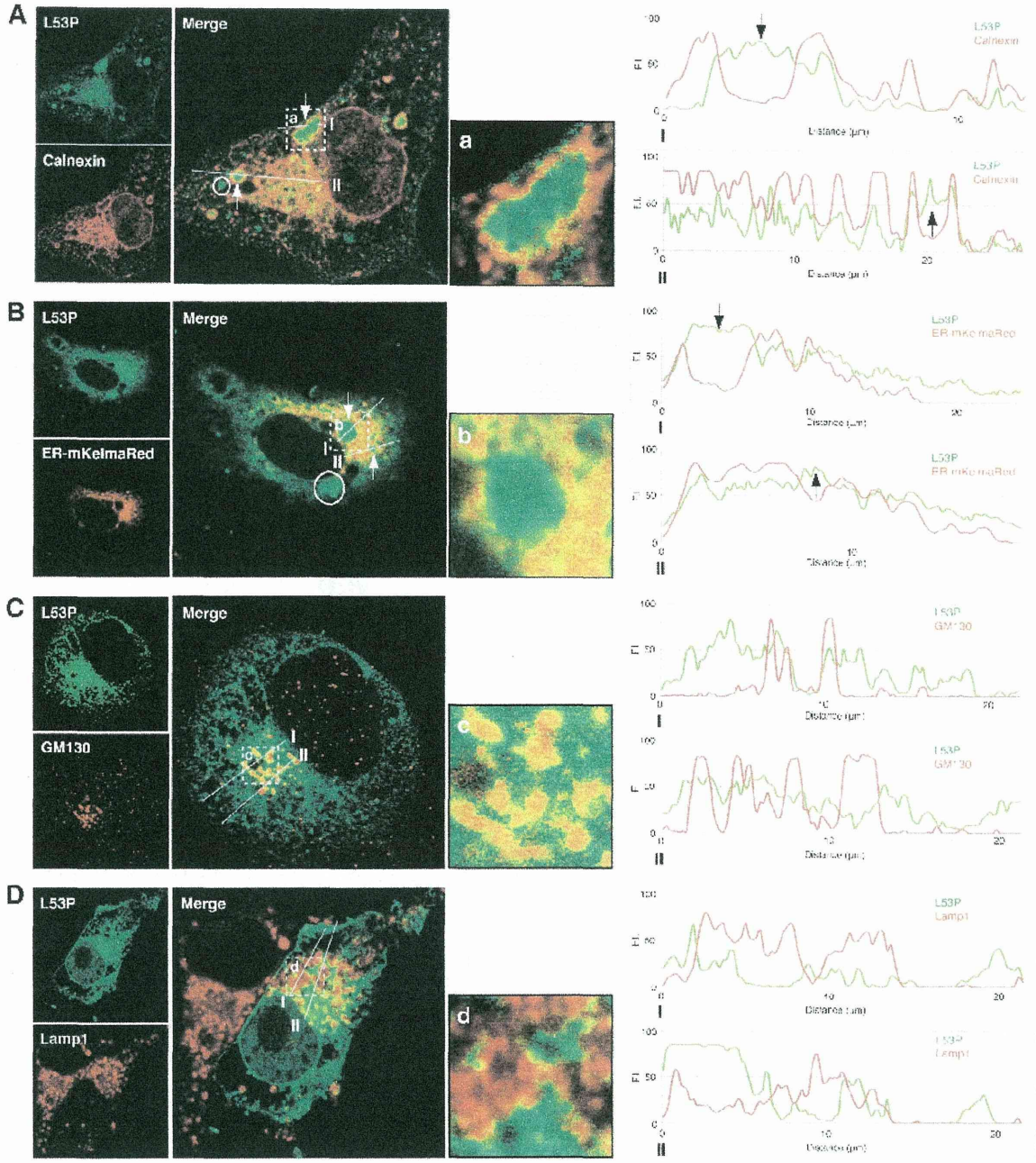

Fig. 3. The L53P mutant accumulates in the endoplasmic reticulum (ER) and Golgi apparatus. Cos-7 cells were transfected with the plasmid encoding FAM126AL53P-EGFP (green) and immunostained with an antibody (red) against the ER marker calnexin (A), the Golgi marker GM130 (C), or the lysosome marker Lamp1 (D). In (B), ER-mKelmaRed was co-transfected. Fluorescence intensity values are shown along lines from perinuclear to peripheral regions. In (A) and (B), arrows and open circles indicate typical large aggregate-like structures surrounded by the ER membrane and those not surrounded by the ER membrane, respectively.

inserted EGFP-tag into the N-terminal position but this construct was not expressed in Cos-7 cells. This may be due to the fact that the N-terminal position of proteins often contains a key organelle localization signal amino acid sequence. Alternatively, EGFP, tagged at the N-terminus, may break FAM126A conformational stability. We thus inserted EGFP-tag into the C-terminus and confirmed FAM126A expression in cells (Fig. 1A). Wild type FAM126A exhibits a broad localization throughout the cytoplasm. While the L53P mutant proteins likely exhibited partial localization in cytoplasmic regions, they were primarily present in punctate structures and were in moderate to large sized aggregates [7,8,15,16]. Cells showing such a localization pattern accounted for ~90% of the transfected cells ($p < 0.01$; n = 120) (Fig. 1B).

We thus tested the hypothesis that the L53P mutation causes FAM126A proteins to aggregate, forming punctate structures in cells. We boiled protein samples from transfected cells in a sample buffer with or without a reducing agent, dithiothreitol, and applied them to SDS-PAGE. As shown in Figure 2, expression of either wild type or mutant exhibited a protein of ~70 kDa after treatment with a sample buffer with the reducing agent. However, in a sample

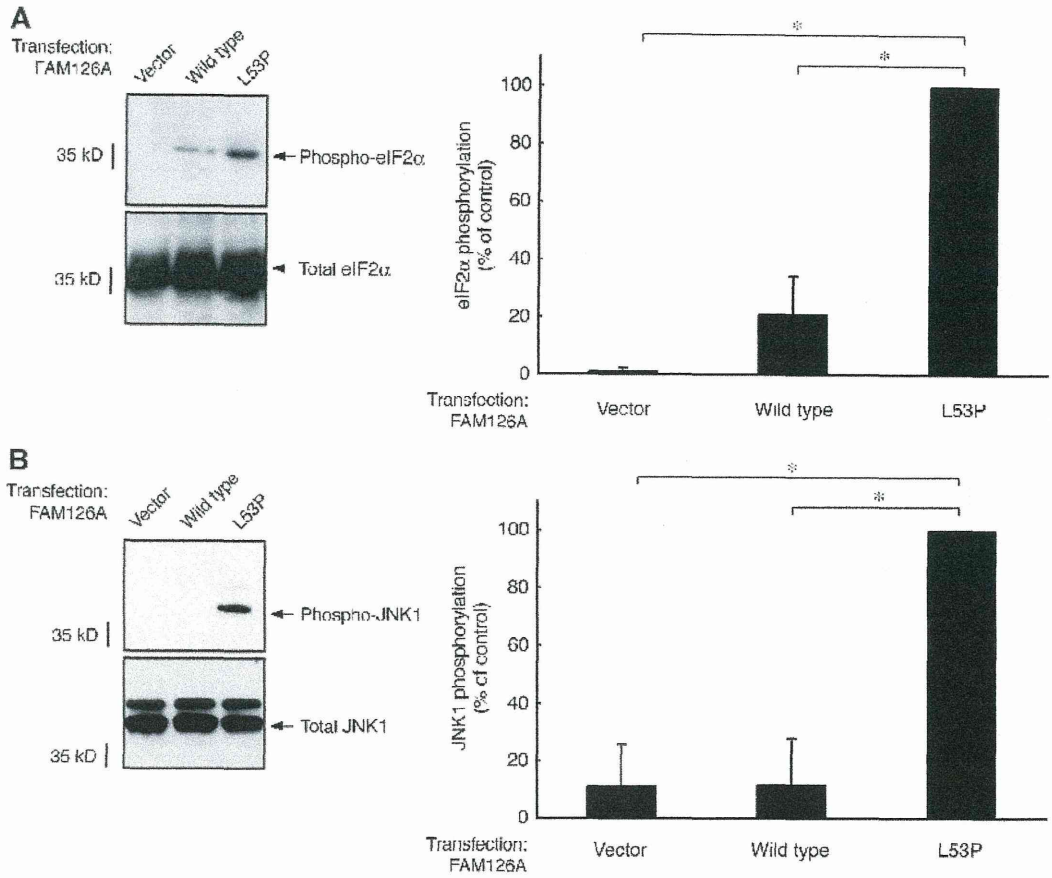

Fig. 4. The L53P mutant stimulates unfolded protein response-responsible kinases. (A) Cos-7 cells were transfected with the plasmid encoding FAM126A-FLAG, FAM126AL53P-FLAG, or vector only and lysed. The lysates were used for immunoblotting with an anti-(pSer51) eIF2α or anti-eIF2α antibody. The band intensities of phosphorylated eIF2α were calculated and are shown as the relative values. (B) The lysates were used for immunoblotting with an anti-(pThr183/Tyr185) JNK or anti-JNK antibody. The band intensities of phosphorylated JNK1 were calculated and are shown as the relative values. *$p < 0.01$ (one way analysis of variance).

buffer without the reducing agent, the wild type protein exhibited a protein of ~70 kDa whereas the mutant had ~40% of its protein in bands at 140 to 150 kDa ($p < 0.01$; $n = 3$), suggesting that the L53P mutation in FAM126A causes protein aggregation with a disulfide bond. The estimated molecular weight of the mutant is ~2-fold higher compared to that of wild type.

3.2. L53P mutant localizes in the ER and Golgi apparatus Cos-7 cells

Next, we determined the subcellular localization of the FAM126A L53P mutant by performing immunofluorescence studies using marker antibodies of organelles including the ER, Golgi apparatus, and lysosomes, where large-sized protein aggregates are often observed [7,8,15,16]. Most of the L53P mutant proteins were localized within an ER membrane stained with an antibody against calnexin, which was consistent with the results of transfection with ER-mKeimaRed (Fig. 3A, B). In addition, the L53P mutant proteins were partially co-localized with a Golgi apparatus marker, GM130 (Fig. 3C). In the graphs, staining intensities measured according to pixel brightness were evaluated through a fluorescence intensity profile of lines I and II using ImageJ software. However, they were not primarily localized in the lysosome, since strong co-localization with the lysosome marker protein, Lamp1, was not observed (Fig. 3D). These results suggest that the L53P mutant proteins form aggregate-like structures in the ER and Golgi apparatus.

3.3. L53P mutant stimulates kinases phosphorylating eIF2α and JNK Cos-7 cells

We thus tested whether the L53P mutant triggers UPR caused by protein aggregation [7,8,17,18]. Three major UPR signaling pathways are known to link to the activation of two types of serine/threonine kinases phosphorylating eIF2α and JNK [7,8,15–18]. To detect eIF2α and JNK phosphorylation, we used antibodies that specifically recognize phosphorylation of eIF2α and JNK. Expression of the L53P mutant resulted in activating eIF2α and JNK phosphorylation (Fig. 4).

3.4. Properties of FAM126A L53P mutant in cells of the mouse brain

To confirm the properties of the L53P mutant in cells of the brain, we established a TG mouse that expressed the L53P mutant of FLAG-tagged FAM126A under the control of an oligodendorocyte-specific MBP promoter (Fig. 5A, B). In TG mouse corpus callosum protein lysates, the L53P mutant protein exhibited a band of ~70 kDa under reducing conditions, whereas it showed probable dimeric bands of ~140 Da under non-reducing conditions, similar to their biochemical properties in Cos-7 cells (Fig. 5C). The L53P mutant protein aggregates were primarily co-localized with the ER marker calnexin but not with the Golgi apparatus marker GM130 in TG mouse corpus callosum cells (Fig. 5D, E), although the size of aggregates seen here was not as large as that in Cos-7 cells. This may be a result of differences in protein tags or cell types

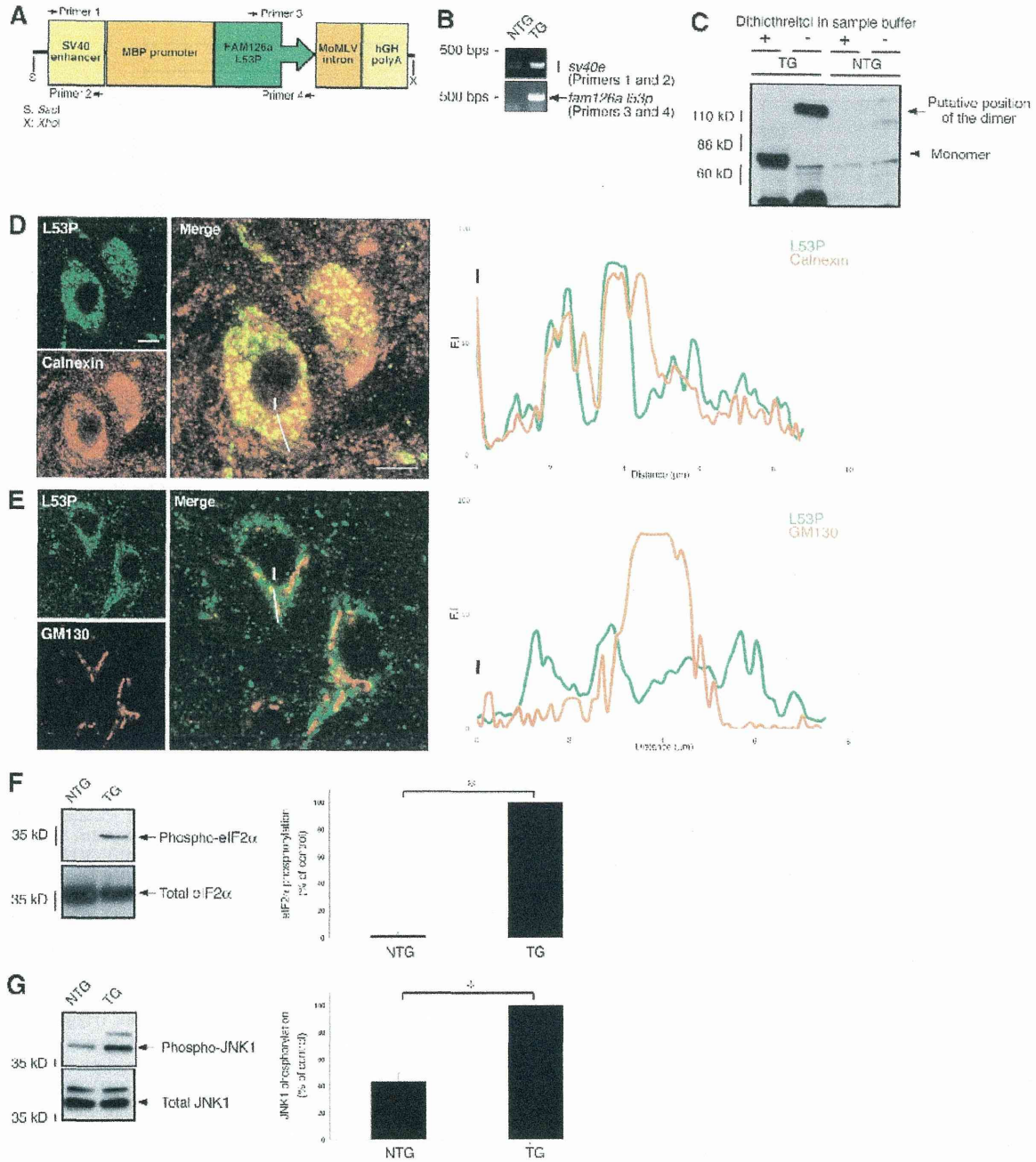

Fig. 5. Analysis of the L53P mutant in cells of mouse brain. (A) Construction of the transgene expressing FAM126AL53P-FLAG. (B) Genomic polymerase chain reaction analysis for the *fam126a* and *sv40* genes using transgenic and non-transgenic littermate control mouse tails. (C) One-month-old mouse corpus callosum was isolated, lysed, and used in immunoblotting of FAM126AL53P-FLAG following SDS-polyacrylamide gel electrophoresis in the presence or absence of dithiothreitol. The sections of transgenic mouse corpus callosum were co-stained with an anti-FLAG antibody (green) and an antibody (red) against the endoplasmic reticulum marker calnexin (D) or the Golgi marker GM130 (E). Fluorescence intensity profiles from position I are also shown. Scale bar = 10 μm. Mouse callosum was isolated, lysed, and used for immunoblotting with anti-(pSer51) eIF2α and anti-eIF2α antibodies (F), or with anti-(pThr183/Tyr185) c-Jun N-terminal kinase (JNK) and anti-JNK antibodies (G). The relative values of bands are also shown. $^{*}p < 0.01$ (one way analysis of variance). eIF2α = eukaryotic translation initiation factor 2α, hGH = human growth hormone, JNK1 = c-Jun N-terminal kinase 1, MBP = myelin basic protein, MoMLV = moloney murine leukemia virus, M130 = Golgi matrix protein 130, NTG = non-transgenic, TG = transgenic.

used. In either case, the L53P mutant seems likely to accumulate in the ER and stimulate eIF2α and JNK phosphorylation, as seen in Cos-7 cells (Fig. 5F, G).

4. Discussion

While recent studies of hereditary hypomyelinating diseases in the CNS identify a number of genes other than *plp1* as disease-responsible genes with various mutations, comparatively less is known about the effect of gene mutations on the biochemical properties of their products [9]. In HLD5, *fam126a* mutations mostly result in a deficiency of FAM126A protein expression. It is thus likely that loss of function of FAM126A is often responsible for pathogenesis of HLD5 [9–12]. Conversely, one unique *fam126a* gene mutation allows some protein to be produced. In this study, we demonstrate that the L53P mutation in FAM126A leads to

FAM126A protein aggregation. This conclusion is supported by biochemical data that suggests that that the L53P mutant proteins exhibit a high molecular weight position in SDS-PAGE under non-reducing conditions; in contrast, in the wild type proteins, the protein band with a high molecular weight position was not detected. In SDS-PAGE under reducing conditions, either the L53P mutant or wild type protein exhibited a predicted molecular weight. In addition, expression of the L53P mutant proteins primarily leads to their accumulation in the ER. It is suggested that changes in the properties caused by the missense mutation of FAM126A are similar to the changes observed for the missense mutations of PLP1 [7,8].

Various types of the *plp1* gene mutations are responsible for the prototypic hereditary hypomyelinating disease HLD1 [1–8]. The pathogenic mechanism in *plp1* missense mutations is believed to begin with the accumulation of mutation-induced, misfolded PLP1 proteins in the ER and/or other organelles on the secretory pathway, triggering an UPR [7,8]. Similarly, FAM126A mutant proteins have the ability to accumulate in the ER and upregulate UPR-responsible kinases. Further studies may clarify whether the similarity of the effects of PLP1 and FAM126A mutations on their properties can explain certain mechanisms by which mutated FAM126A proteins lead to hypomyelination.

PLP1 is transported into the plasma membrane and is a required constituent of the myelin membrane. PLP1 missense mutations, in addition to triggering an UPR, result in aberrant PLP1 protein localization, which leads to a functional deficiency. Mutated PLP1 proteins are mostly present on the secretory pathway and are not localized at the myelin membrane where normal PLP1 should function [1–3]. This is also thought to be one of the reasons why PLP1 mutations cause hypomyelination. Our study suggests that wild type FAM126A protein is localized in the cytoplasm, whereas the mutant is, at least in part, present in the ER. It is conceivable that the FAM126A missense mutation causes aberrant location within the cell, possibly causing a partial decrease in the cellular activities in the affected cytoplasmic regions.

The cellular function of FAM126A is largely unknown. FAM126A is probably a cytoplasmic protein. Indeed, public bioinformatics websites such as the SOSUI program predict that FAM126A is a soluble protein. FAM126A has no typical transmembrane domain, such as the one characterized by sequential hydrophobic amino acids. In agreement with this prediction, FAM126A contains many highly-probable phosphorylation sites (see the NetPhos bioinformatics website), which generally exist in the intracellular region, but FAM126A does not contain a potential N-glycosylaton site (see the NetNGlyc bioinformatics website), which exists in the extracellular region. A recent study identified the SIMPLE gene product, which has been an unknown cytoplasmic protein responsible for demyelinating Charcot-Marie-Tooth disease in the peripheral nervous system, as a cytoplasmic protein required for recruitment of the endosomal sorting complex required to transport components to endosomal membranes [19]. FAM126A may be such a protein in the CNS. Further studies will increase our understanding of how the L53P mutant protein accumulation occurs in primary cells such as oligodendrocytes and other cells in the CNS [12]. Such studies may reveal a common molecular mechanism underlying the relationship between hereditary hypomyelinating diseases and the related missense mutations.

Conflicts of Interest/Disclosures

The authors declare that they have no financial or other conflicts of interest in relation to this research and its publication.

Acknowledgements

We thank Drs. J.R. Chan, N. Kitamura, and E.M. Shooter for helpful discussions. This work was supported by Grants-in-Aid for Scientific Research from the Japanese Ministry of Education, Culture, Sports, Science, and Technology (MEXT) and the Japanese Ministry of Health, Labour, and Welfare (MHLW). This work was also partially supported by grants from the Kanehara Foundation, the Kowa Foundation, the Mochida Foundation, the Naito Foundation, and the Takeda Foundation.

References

[1] Nave KA, Trapp BD. Axon-glial signaling and the glial support of axon function. Annu Rev Neurosci 2008;31:535–61.
[2] Garbern J, Cambi F, Shy M, et al. The molecular pathogenesis of Pelizaeus-Merzbacher disease. Arch Neurol 1999;56:1210–4.
[3] Garbern JY. Pelizaeus-Merzbacher disease: genetic and cellular pathogenesis. Cell Mol Life Sci 2007;64:50–65.
[4] Kagawa T, Ikenaka K, Inoue Y, et al. Glial cell degeneration and hypomyelination caused by overexpression of myelin proteolipid protein gene. Neuron 1994;13:427–42.
[5] Klugmann M, Schwab MH, Pühlhofer A, et al. Assembly of CNS myelin in the absence of proteolipid protein. Neuron 1997;18:59–70.
[6] Gow A, Southwood CM, Lazzarini RA. Disrupted proteolipid protein trafficking results in oligodendrocyte apoptosis in an animal model of Pelizaeus-Merzbacher disease. J Cell Biol 1998;140:925–34.
[7] Southwood CM, Garbern J, Liang W, et al. The unfolded protein response modulates disease severity in Pelizaeus-Merzbacher disease. Neuron 2002;36:585–96.
[8] Dhaunchak AS, Colman DR, Nave KA. Misalignment of PLP/DM20 transmembrane domains determines protein misfolding in Pelizaeus-Merzbacher disease. J Neurosci 2011;31:14961–71.
[9] Hobson GM, Garbern JY. Pelizaeus-Merzbacher disease, Pelizaeus-Merzbacher-like disease 1, and related hypomyelinating disorders. Semin Neurol 2012;32:62–7.
[10] Zara F, Biancheri R, Bruno C, et al. Deficiency of hyccin, a newly identified membrane protein, causes hypomyelination and congenital cataract. Nat Genet 2006;38:1111–3.
[11] Ugur SA, Tolun A. A deletion in DRCTNNB1A associated with hypomyelination and juvenile onset cataract. Eur J Hum Genet 2008;16:261–4.
[12] Gazzerro E, Baldassari S, Giacomini C, et al. Hyccin, the molecule mutated in the leukodystrophy hypomyelination and congenital cataract (HCC), is a neuronal protein. PLoS ONE 2012;7:e32180.
[13] Miyamoto Y, Torii T, Tanoue A, et al. Pelizaeus-Merzbacher disease-associated proteolipid protein 1 inhibits oligodendrocyte precursor cell differentiation via extracellular-signal regulated kinase signaling. Biochem Biophys Res Commun 2012;424:262–8.
[14] Yamauchi J, Miyamoto Y, Torii T, et al. Phosphorylation of cytohesin-1 by Fyn is required for initiation of myelination and the extent of myelination during development. Sci Signal 2012;5:ra69.
[15] Liu N, Yamauchi J, Shooter EM. Recessive, but not dominant, mutations in peripheral myelin protein 22 gene show unique patterns of aggregation and intracellular trafficking. Neurobiol Dis 2004;17:300–9.
[16] Ryan MC, Shooter EM, Notterpek L. Aggresome formation in neuropathy models based on peripheral myelin protein 22 mutations. Neurobiol Dis 2002;10:109–18.
[17] Taveggia C, Feltri ML, Wrabetz L. Signals to promote myelin formation and repair. Nat Rev Neurol 2010;6:276–87.
[18] Pereira JA, Lebrun-Julien F, Suter U. Molecular mechanisms regulating myelination in the peripheral nervous system. Trends Neurosci 2012;35:123–34.
[19] Lee SM, Chin LS, Li L. Charcot-Marie-Tooth disease-linked protein SIMPLE functions with the ESCRT machinery in endosomal trafficking. J Cell Biol 2012;199:799–816.

Biochemical and Biophysical Research Communications 452 (2014) 782–788

Contents lists available at ScienceDirect

Biochemical and Biophysical Research Communications

journal homepage: www.elsevier.com/locate/ybbrc

In vivo knockdown of ErbB3 in mice inhibits Schwann cell precursor migration

Tomohiro Torii [a,1], Yuki Miyamoto [a,1], Shuji Takada [b,d], Hideki Tsumura [c], Miyuki Arai [c], Kazuaki Nakamura [a], Katsuya Ohbuchi [e], Masahiro Yamamoto [e,f], Akito Tanoue [a], Junji Yamauchi [a,d,*]

[a] Department of Pharmacology, National Research Institute for Child Health and Development, Setagaya, Tokyo 157-8535, Japan
[b] Department of Systems BioMedicine, National Research Institute for Child Health and Development, Setagaya, Tokyo 157-8535, Japan
[c] Laboratory Animal Facility, National Research Institute for Child Health and Development, Setagaya, Tokyo 157-8535, Japan
[d] Graduate School of Medical and Dental Sciences, Tokyo Medical and Dental University, Bunkyo, Tokyo 113-8510, Japan
[e] Tsumura Research Laboratories, Tsumura & Co., Inashiki, Ibaraki 200-1192, Japan
[f] School of Medicine, Keio University, Shinjuku, Tokyo 160-8583, Japan

ARTICLE INFO

Article history:
Received 25 August 2014
Available online 6 September 2014

Keywords:
ErbB3
In vivo knockdown
Mouse
Schwann cell precursor
Migration

ABSTRACT

The myelin sheath insulates neuronal axons and markedly increases the nerve conduction velocity. In the peripheral nervous system (PNS), Schwann cell precursors migrate along embryonic neuronal axons to their final destinations, where they eventually wrap around individual axons to form the myelin sheath after birth. ErbB2 and ErbB3 tyrosine kinase receptors form a heterodimer and are extensively expressed in Schwann lineage cells. ErbB2/3 is thought to be one of the primary regulators controlling the entire Schwann cell development. ErbB3 is the *bona fide* Schwann cell receptor for the neuronal ligand neuregulin-1. Although ErbB2/3 is well known to regulate both Schwann cell precursor migration and myelination by Schwann cells in fishes, it still remains unclear whether in mammals, ErbB2/3 actually regulates Schwann cell precursor migration. Here, we show that knockdown of ErbB3 using a Schwann cell-specific promoter in mice causes delayed migration of Schwann cell precursors. In contrast, littermate control mice display normal migration. Similar results are seen in an *in vitro* migration assay using reaggregated Schwann cell precursors. Also, ErbB3 knockdown in mice reduces myelin thickness in sciatic nerves, consistent with the established role of ErbB3 in myelination. Thus, ErbB3 plays a key role in migration, as well as in myelination, in mouse Schwann lineage cells, presenting a genetically conservative role of ErbB3 in Schwann cell precursor migration.

1. Introduction

In the embryonic stages of peripheral nervous system (PNS) development, Schwann cell precursors migrate along neuronal axons to their final destinations. After birth, Schwann cells wrap around individual axons, forming myelin sheaths. The myelin sheath is a morphologically differentiated Schwann cell plasma membrane that insulates axons and markedly increases the nerve conduction velocity. It also plays a role in protecting axons from various external factors such as physical stresses [1,2].

Many growth factors and adhesion molecules, which are derived from peripheral neurons, bind to cognate receptors that are expressed in Schwann cells, and thereby regulate certain processes involved in the myelination of axons [3–6]. Among these ligand–receptor interactions, the relationship between axonal neuregulin-1 (NRG1) type III variant and Schwann cell ErbB2/3 heterodimeric receptor is thought to be one of the primary units controlling Schwann cell development. In the PNS, NRG1 is specifically expressed in neurons and ErbB2/3 is specifically expressed in Schwann cells. NRG1 binds to ErbB3, whose structural change stimulates ErbB2 tyrosine kinase, to activate an array of intracellular signaling cascades. ErbB3 has a very low tyrosine kinase activity and ErbB2 has little ligand-binding activity [3,4]. It is well established that in zebrafish, Schwann cell ErbB2/3 receptor is critical not only for achieving myelination of posterior lateral line axons but also for regulating Schwann cell precursor migration [5]. In a series of mouse genetic studies, the ErbB2/3 receptor has also been

* Corresponding author at: Department of Pharmacology, National Research Institute for Child Health and Development, 2-10-1 Okura, Setagaya, Tokyo 157-8535, Japan. Fax: +81 3 5494 7057.
E-mail address: yamauchi-j@ncchd.go.jp (J. Yamauchi).
[1] These authors equally contributed to this work.

http://dx.doi.org/10.1016/j.bbrc.2014.08.156
0006-291X/

shown to play an essential role in PNS myelination [2–4]; however, the important question of whether the mammalian ortholog is actually involved in the migration of Schwann cell precursors still remains to be answered.

In this study, we have produced transgenic mice transcribing ErbB3 short-hairpin RNA (shRNA)-inserted artificial microRNA (miRNA) [7,8] under the control of a Schwann cell-specific myelin protein zero (MPZ, also called P0) promoter and found that knockdown of ErbB3 *in vivo* results in delayed migration of Schwann cell precursors. Also, shErbB3 transgenic mice exhibit reduced myelin thickness, as seen in studies using knockout mice. Therefore, signaling through the *erbb3* gene product is required for Schwann cell precursor migration, indicating that the role of the ErbB3 receptor in fish Schwann cell precursor migration is conserved in mammals.

2. Materials and methods

2.1. Antibodies

The following antibodies were purchased: polyclonal anti-ErbB2 and anti-ErbB3, and monoclonal anti-Ki67 antigen from Cell Signaling Technology (Danvers, MA, USA); polyclonal anti-Sox10 (Schwann cell lineage cell's marker) from Santa Cruz Biotechnology (Santa Cruz, CA, USA); polyclonal anti-p75 neurotrophin receptor (Schwann cell marker) from Promega (Madison, WI, USA); monoclonal anti-myelin basic protein (MBP) from Covance (Princeton, NJ, USA); monoclonal anti-actin from MBL (Nagoya, Japan); and peroxidase-conjugated secondary antibodies from Nacalai Tesque (Kyoto, Japan) or Wako (Osaka, Japan). Fluorescence-labeled secondary antibodies were obtained from Nacalai Tesque or Life Technologies (Carlsbad, CA, USA).

2.2. Cultures and migration assays of Schwann cell precursors

Primary Schwann cell precursors were prepared from dorsal root ganglia (DRGs) of male or female C57BL/6J mice on embryonic day 12.5 and cultured at 37 °C as previously described [9,11]. For migration assay, cell reaggregates were allowed to migrate in Sato medium containing 10 ng/ml NRG1 (R&D Systems, Minneapolis, MN, USA) on type I collagen-coated dishes or wells for 6 h [12]. The maximum distance from the center of the reaggregate was considered the migrating distance. To confirm cell viability under these experimental conditions, cells were stained with 0.4% trypan blue. Stained cells routinely accounted for less than 5% of all cells.

2.3. Schwann cell-neuronal cultures

Dissociated explants were established from male or female mice on embryonic day 12.5 [9,10]. In brief, DRGs were collected and dissociated using 0.25% trypsin and trituration. The cells were dispersed and plated onto collagen-coated coverslips (3×10^5 cells/22 mm-coverslip). The dissociated explants were maintained in MEM containing 10% FBS and 100 ng/ml NGF. Axonal processes and endogenous Schwann cells were allowed to grow and establish themselves for 5 days. Myelination was induced using 50 μg/ml ascorbic acid. The culture medium was changed every 2 or 3 days and cultures were maintained for an additional 2 weeks.

2.4. Generation of Schwann cell-specific shErbB3 transgenic mice

The mouse MPZ promoter (GenBank Acc. No. M62857) was amplified using C57BL/6J mouse genomic DNAs. Mouse ErbB3 shRNAs, designed using an RNAi Design program (http://rnaidesigner.lifetechnologies.com/rnaiexpress/), were inserted into the BLOCK-iT PolII miR RNAi expression vector (Cat. No. K4936-00; Life Technologies), followed by amplification with the 704-2010 bases. The ErbB3 nucleotide target sequences used were 5′-TACCC ATGACCACCTCACACT-3′ (ErbB3's 164-184 bases) and 5′-ATATCT GGCAGTCTTCTGGTC-3′ (ErbB3's 593-613 bases). The nucleotides encoding the promoter, shRNA-inserted artificial miRNA, and polyA signal units were successively inserted into the pCMV5 backbone as the subcloning vector. A DNA fragment (~2.7-kb) containing all nucleotide units was digested from the vector backbone with *Eco*RI and *Pst*I, purified, and injected into fertilized C57BL/6J oocytes [9,10]. Transgenic founder mice and established transgenic mice were identified by tail DNA's genomic PCRs with specific primers (5′-ATGGTGAGCAAGGGCGAGGAGCTG-3′ and 5′-CTTGTAC AGCTCGTCCATGCCGAGAGTGATC-3′ for the artificial miRNA sequence; 5′-GCTAACTGAAACACGGAAGGAGACAATACCGGAAG-3′ and 5′-CAGCTGCGCAGATCCATCAGAGATTTTGAGAC-3′ for the polyA sequence; and 5′-GTTGAAAATTGTGGATACTTTGACAC-3′ and 5′-TGAAGGGACATCTAACTACAATCAA-3′ for the *arf1* gene as the internal control), as well as by Southern blotting with *Hin*dIII-digested tail DNA hybridized to a radioisotope-labeled genomic probe for the artificial miRNA. The transgenic allele resulted in a hybridized band of ~1.4 kb. The scanned bands were densitometrically analyzed to identify their semi-quantification using an UN-SCAN-IT gel software (Silk Scientific, Orem, UT, USA). PCR was performed in 30 cycles, each consisting of denaturation at 94 °C for 1 min, annealing at 55–65 °C (depending on each primer's Tm value) for 1 min, and extension at 72 °C for 1 min. Transgenic founders were mated to wild type C57BL/6J mice and the transgene was stably maintained for at least 4 generations. The transgenic mice were fertile under standard breeding conditions. Male mice were used for experiments if it was possible to distinguish their sex.

2.5. Immunoblotting

Cells were lysed in lysis buffer A (50 mM HEPES-NaOH, pH 7.5, 20 mM $MgCl_2$, 150 mM NaCl, 1 mM dithiothreitol, 1 mM phenylmethane sulfonylfluoride, 1 μg/ml leupeptin, 1 mM EDTA, 1 mM Na_3VO_4, and 10 mM NaF) containing biochemical detergents (0.5% NP-40, 1% CHAPS, and 0.3% SDS). Unless otherwise indicated, all lysis steps were performed at 4 °C [9,10]. The proteins in the cell supernatants were denatured, subjected to SDS–PAGE, and blotted to a polyvinylidene difluoride membrane using the TransBlot Turbo Transfer System (Bio-Rad, Hercules, CA, USA). The membranes were blocked with a Blocking One reagent (Nacalai Tesque), and immunoblotted using a primary antibody followed by a peroxidase-conjugated secondary antibody. The bound antibodies were detected using the chemiluminescence method (Nacalai Tesque or Wako) and scanned bands were analyzed densitometrically.

2.6. Immunofluorescence

Cells on dishes or wells were fixed in PBS containing 4% paraformaldehyde and permeabilized with PBS containing 0.1% Tween-20. Permeabilized cells were blocked with Blocking One, and incubated first with primary antibodies and then with fluorescence-labeled secondary antibodies. They were mounted for microscopic observation using Vectashield Mounting Medium (Vector Laboratories, Burlingame, CA, USA). The fluorescent images were captured using a DMI4000 or DMI4000B microscope system (Leica, Wetzlar, Germany) and analyzed using AF6000 software (Leica).

2.7. Immunohistochemistry

Tissues were perfused first with PBS and then with PBS containing 4% paraformaldehyde. They were postfixed with 4%

paraformaldehyde, replaced with 20% sucrose, and embedded in Tissue-Tek reagent (Sakura Finetechnical, Tokyo, Japan). Microtome sections were blocked with Blocking One, and incubated first with primary antibodies and then with fluorescence-labeled secondary antibodies. The glass coverslips were mounted with Vectashield. The fluorescent images were captured using a DM2500 microscope system (Leica) and analyzed using LAS software (Leica) or captured using a BX51 microscope system (Olympus, Tokyo, Japan) and analyzed using DP2-BSW software (Olympus).

2.8. Electron microscopy

Tissues were fixed with 2% paraformaldehyde and 2% glutaraldehyde in 0.1% cacodylate buffer, contrasted with 2% osmium tetroxide, dehydrated with an ethanol gradient, and treated with propylene oxide. Finally, samples were infiltrated and embedded in pure epoxy. Ultrathin sections were stained with uranyl acetate and lead staining solution. Images were taken with a JEM-1200EX electron microscope system (JEOL, Tokyo, Japan). The g-ratio is the value of axon diameter to outer myelinated axon diameter.

2.9. Ethics statement

Genetically modified/unmodified mice were produced and maintained in accordance with a protocol approved by the Japanese National Research Institute for Child Health and Development Animal Care Committee.

2.10. Statistical analysis

Values shown represent the mean ± SD from separate experiments. One-way analysis of variance (ANOVA) was performed followed by a Fisher's protected least significant difference (PLSD) test as a post hoc comparison. A p value less than 0.01 was considered significant.

3. Results

The aim of this study was to determine whether the ErbB3 receptor regulates Schwann cell precursor migration in mammals. Therefore, we injected a linearized transgene containing the shRNA sequence for ligand-binding ErbB3 receptor under the control of a MPZ promoter into fertilized mouse eggs, according to the standard method of transgenic mouse production (Fig. 1A). The shErbB3 nucleotide sequence is inserted within an miRNA backbone and is transcribed as artificial miRNA in an MPZ promoter-dependent manner. This knockdown construct is often called shRNAmir [7,8]. MPZ promoter is active in Schwann cell lineage cells [13,14]. We succeeded in generating three founder mice, each harboring multiple transgenes, which were mated to wild type mice. In only one transgenic line, the transgene was stably maintained for several

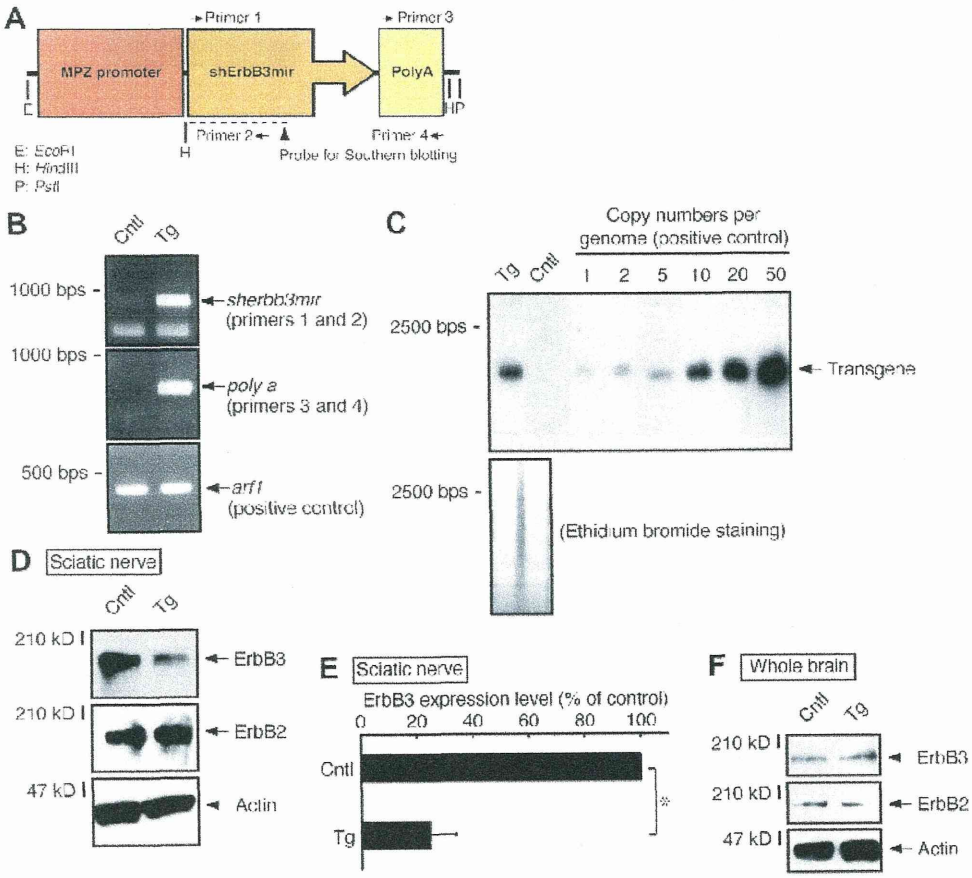

Fig. 1. Knockdown effect of ErbB3 in shErbB3 transgenic mice. (A) Schematic diagram of the shErbB3mir transgene. The positions of genomic PCR primers (arrows), Southern blotting probe (dashed lines), and restriction enzymes (single large characters) are shown. (B) Representative genomic PCR photographs for control mice (Cntl) and transgenic mice (Tg) are shown. The *arf1* gene is the positive genomic PCR control. (C) Genomic DNAs were digested with *HindIII* and Southern blotting was performed using radioisotope-labeled shErbB3mir fragments as the probe. The number of transgene copies (~10 copies) per genome was measured in comparison with that in positive control fragments. Ethidium bromide staining is also shown. (D and E) Immunoblottings for ErbB receptors and control actin were performed using sciatic nerve tissue lysates. ErbB3 bands were scanned and their relative intensities are statistically shown (*$p < 0.01$; $n = 3$). (F) Immunoblots for ErbB receptors and actin using whole brain lysates are shown.